

# Evaluation of Biochar Production Temperature in Interaction with Elastomers of Different Polarities

William B. Ribeiro<sup>a</sup> , Giovanni B. Bérti<sup>a</sup>, Máira Faccio<sup>b</sup> , Marcelo Godinho<sup>a</sup>,  
Rosmary N. Brandalise<sup>a\*</sup> 

<sup>a</sup>Universidade de Caxias do Sul (UCS), Programa de Pós-Graduação em Engenharia de Processos e Tecnologias (PGEPROTEC), 95070-560, Caxias do Sul, RS, Brasil.

<sup>b</sup>Universidade de Caxias do Sul (UCS), Programa de Pós-Graduação em Engenharia e Ciência dos Materiais (PPGMAT), 95070-560, Caxias do Sul, RS, Brasil.

Received: July 29, 2022; Revised: November 03, 2022; Accepted: December 01, 2022

The present work is to study the production and characterization of biochar produced at two different temperatures (400 and 900 °C) and its influence on the interaction of biochar with elastomers of different polarity, aiming at the replacement of carbon black in elastomer compounds, based on the rheometric, physical, chemical and mechanical properties. The biochar production temperature of 900 °C affected the optimum vulcanization time ( $t_{90}$ ), with compounds containing NR and NBR having the shortest vulcanization times because temperatures above 400 °C produce an alkaline biochar that accelerates vulcanization. The biochar interacted with the two elastomers, being superior to NBR due to the oxygen concentration. Therefore, the blends with biochar showed a demonstrated reinforcement of the tensile strength, even if the biochar had a surface area of 3 m<sup>2</sup>.g<sup>-1</sup> for the observed irregular surface, in addition to the mechanical properties, analogous to the blends with carbon black.

**Keywords:** *Interaction, polarity, biochar, carbon black, pyrolysis.*

## 1. Introduction

Elastomeric compounds are used in a wide variety of everyday applications, such as tires, seals, biomaterials, and many others, due to their suitable dynamic mechanical, physical, and mechanical properties. These properties depend on the formulation of the elastomer, and in any formulation, there must be a synergistic effect between all the components and their quantities. Reinforcing fillers, such as carbon black and silica, give elastomer compounds the physical, mechanical and degradation resistance properties required for saleable applications. The production and use of these fillers can have a negative impact on both the environment and health, as they contain toxic substances adsorbed on their structure<sup>1</sup>.

To reinforce elastomers, the fillers must interact with the elastomer based on their chemical and physical parameters. The key parameters that determine the reinforcing capacity of elastomeric compounds are the size and distribution of the primary particles, the shape (complexity) and distribution of the aggregates, and the surface activity, which is chemically related to the reactivity of the surface functional groups and physicochemically represents the adsorption capacity. The surface free energy determines this capability and the energy distribution on the surface<sup>2</sup>. During mixing between an elastomer and a reinforcing filler, strong interactions take place, the filler-elastomer interaction, which leads to the formation of the bonded rubber, associated with the chemical adsorption process. In addition, there is physical

adsorption, where the isolated aggregates limit the mobility of the chains<sup>3</sup>.

Carbon black is considered one of the most commonly used reinforcing fillers and consists of a polynuclear carbon structure. It contains nanometric particles and is produced by the partial combustion of heavy hydrocarbons. European legislation restricts the marketing of products containing polycyclic aromatic hydrocarbons (PAH) with more than 1 ppm of any of the 8 types of carcinogens PAH. For toys and children's articles, the level is lowered to 0.5 ppm, which makes it difficult to continue using traditional components of the rubber industry, such as carbon black<sup>4</sup>. Therefore, the search for alternative materials and understanding their interaction with rubber is crucial to map the losses and completely replace carbon black, achieving new results in this field. To replace carbon black, the substitutes must have particles between 25 and 500 nm in size, as well as functional groups and a morphology suitable for interaction with the elastomer<sup>5,6</sup>.

The genus *Pinus*, one of the most significant representatives of coniferous trees, is foreordained to manufacture cellulose, furniture, sawmills, natural wood, civil construction, charcoal, steel, and wood panels<sup>7</sup>. Along the *Pinus* wood production process in 2016, is important to highlight the generation of about 47.8 million tons of waste, and its reuse was approximately 52%. With the growing environmental concern, wood residues trace a new path in their use<sup>8</sup>. The high content of volatile matter and low ash content, characteristic of conifers, make them attractive for pyrolysis<sup>7</sup>.

\*e-mail: [mbranda@ucs.br](mailto:mbranda@ucs.br)

Pyrolysis is a thermochemical process that allows the conversion of biomass into a possible reinforcing filler with chemical properties that can favor interaction with elastomers of various types, similar to carbon black, with the advantage of being derived from a renewable resource and presenting a lower PAH concentration<sup>9</sup>. Biochar produced by the pyrolysis of biomass presents itself as a solid, porous product with a disordered molecular structure composed of aromatic rings randomly linked together. The surface chemistry of biochar changes depending on the raw material and the operating parameters used. The organic fraction contains a high carbon content, partly in the amorphous and partly in the crystalline (graphene-like) phase, while the inorganic fraction contains mainly Ca, K, Mg and inorganic carbonates<sup>9</sup>.

Several studies have already shown that biochar reinforces elastomeric compounds<sup>10-14</sup>, although the ability for biochar to interact with elastomers, a fundamental requirement to be considered a reinforcing strain, requires further study. Examining the interaction between biochar and elastomers with different polarities could allow the relationships between the parameters of the pyrolysis process and the mixing process to be accurately determined to improve the reinforcing charge. From the interaction point of view, the current studies on biochar as a reinforcing filler in elastomer compounds are in agreement with the findings on carbon black in 1907.

Considering the possibility of producing biochar from the pyrolysis of *Pinus* spp. and the influence of this process parameter (pyrolysis temperature at 400 and 900 °C) on the properties of biochar, the present work aims to evaluate the biochar-elastomers interaction of different polarities, NR (nonpolar) and NBR (polar), in the substitution of carbon black in elastomeric compositions, based on the bound rubber content and rheometric, physical and mechanical properties.

## 2. Experiment

### 2.1. Materials

GEB type Poly(cis-1,3-isoprene)(NR) was provided by Braslatex; NBR type 615B, with 33% Acrylonitrile by Nitriflex SA; carbon black N550, from CABOT Corporation; zinc oxide from Agrozinco Indústria e Comércio LTDA; stearic acid from Proquitech Indústria de Produtos Químicos AS. Benzothiazyl disulfide (MBTS) is from Interquímica Comércio e Indústria de Produtos Químicos LTDA., n-tert-butyl-2 benzothiazolsulfenamide (TBBS) is from Interquímica Comércio e Indústria de Produtos Químicos LTDA; insoluble sulfur is from Basile Química Indústria e Comércio LTDA; toluene is from Vetec, with 99.9% purity; pure acetone, from Simoquímica. For the pyrolysis process, pellets of wood residue from *Pinus* spp. the Pioaquece branded by Piomade; isopropyl alcohol, from Dinâmica Química Contemporânea LTDA.

### 2.2. Pyrolysis process

The pyrolysis process was carried out in a fixed-bed bench-top reactor operating in batch mode. The system (Figure 1) consists of a Sanchis furnace containing an internally coupled stainless steel reactor. The reactor was

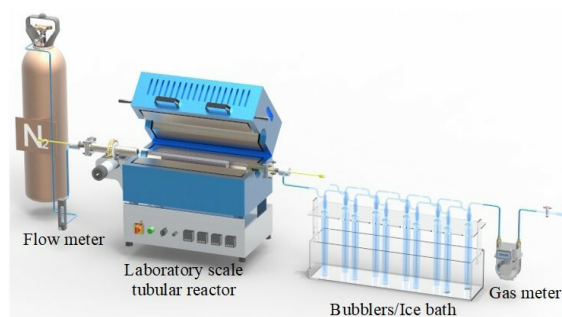


**Figure 1.** Equipment and accessories that integrate the pyrolysis process system.

electrically heated by resistors of 1900 W each, with two type K thermocouples placed inside the reactor (inlet and outlet of the reactor). The condensation of the vapors in bio-oil was carried out according to the adaptation of the standard CEN/TS 15439 using ten bubbles arranged in series, impingers, with 100 mL of isopropyl alcohol in each bubble, except for the first and last, which were empty. The biomass pyrolysis experiments were performed at 400 °C and 900 °C<sup>15</sup> with a residence time of 30 minutes and an inert gas flow ( $N_2$ ) of 200 mL.min<sup>-1</sup> until a mass of biochar was obtained for the preparation of elastomeric compounds. The biochar coding is: BIO400 for the biochar produced at 400 °C and BIO900 for the biochar produced at 900 °C.

### 2.3. Characterization of the produced biochar

The biochar produced at 400 °C and 900 °C was ground in a Retsch planetary ball mill, model Emax (Germany), with 50 mL tungsten carbide vessels and 4.0 mm and 3.0 mm in diameter. The following parameters were used for the grinding process: Mass ratio (m/m) between biochar and spheres of 4.5, agitation speed of 575 rpm for 30 minutes<sup>16</sup>. The following methods were used to characterize the biochar: Proximate analysis, scanning electron microscopy (SEM), surface analysis by  $N_2$  adsorption (BET), and surface free energy by the contact angle method.

Tests for proximate analysis of biochar were performed on a Netzsch STA 449 F3 Jupiter, according to ASTM D7582-15. The experiments included 3 steps: drying, elimination of volatile matter in an inert atmosphere, and combustion in air. Moisture content was considered as mass loss when heating the sample to 110 °C, at a flow rate of 50 mL.min<sup>-1</sup> and a heating rate of 20 °C.min<sup>-1</sup> to constant mass. Then, the elimination of volatile matter step started with a heating rate of 40 °C.min<sup>-1</sup> to 900 °C until a constant mass was reached. Finally, the atmosphere was changed to an air flow rate of 50 mL.min<sup>-1</sup>, keeping the temperature at 900 °C until a constant mass was reached.

The morphological information of the biochar was obtained by means of scanning electron microscopy (SEM) in a JEOL equipment, model JSM 6060 (Japan) with an acceleration voltage of 10 kV. The samples received a thin layer of gold (Au) for further analysis.

The biochar surface area analysis test by  $N_2$  adsorption was determined by the adsorption isotherm method by the Brunauer-Emmet-Teller (BET) method, according to ASTM

D6556-19. The samples were submitted to an elimination of volatile matter procedure to remove interferents in the sample. Afterwards, the adsorption-desorption process in nitrogen took place, following the BET method.

The biochar surface free energy test using the contact angle was performed using the sessile drop method<sup>17</sup>. The samples were shaped into a disk by compression molding. The liquids selected for the study were distilled water and toluene. To obtain information on the surface properties of the biochar, the analysis of the surface free energy was performed with the London dispersive component and the specific polar component by the Fowkes method<sup>17</sup>. The surface and droplet images were acquired with a camera digital brand Panasonic. SurfTens software was used to determine the contact angle.

#### 2.4. Preparation of the elastomeric composites

ASTM D3192-09 was adopted for the base formulation of NR, and the following amounts in phr were held constant for all samples: NR - 100, ZnO - 5, stearic acid - 3, charge - 50, sulfur - 2.5, MBTS - 0.6. For the base formulation of NBR, ASTM D3848-03 was adopted, and the following amounts in phr were held constant for all samples: NBR - 100, ZnO - 3, stearic acid - 1, charge - 50, sulfur - 1.5, TBBS - 0.7.

The elastomeric formulations were initially processed in a handcrafted torque rheometer that resembles a Haake type, with a useful mixing chamber volume of 65 cm<sup>3</sup>. The mixtures were produced at 100 °C, 60 rpm and a processing time of 10 minutes, with elastomer, activators and filler being added. After resting for 24 h, the premix carried out in the torque rheometer was added in a two-roll mill (MH-600 - Brazil) at 60 °C, with the accelerator and sulfur being added to the premix.

The encoding used for the elastomeric compounds was: (NR) for uncharged NR compound; (NR/CB) for NR compound with carbon black; (NR/BIO400) for NR compound with biochar produced at 400°C; (NR/BIO900) for NR compound with biochar produced at 900°C. The same was adopted for NBR, with only the rubber acronym being changed (NBR, NBR/CB, NBR/BIO400 and NBR/BIO900).

#### 2.5. Characterization of elastomeric compounds

The elastomeric compounds were characterized after mixing in the torque mixer by testing the bonded rubber content. The bound rubber content<sup>18</sup> was quantified from the extraction of the elastomeric compound with toluene solvent for NR and acetone for NBR. Samples of approximately 1 g were immersed in 200 mL of solvent at 25°C for 45 h. Afterward, they were oven-dried to constant mass<sup>18</sup>. The bound rubber content was calculated according to Equation 1.

$$BR = \frac{W_{fg} - W_t \left[ \frac{m_f}{(m_f + m_r)} \right]}{W_t \left[ \frac{m_r}{(m_f + m_r)} \right]} \cdot 100 \quad (1)$$

Where BR is the bound rubber content (%);  $W_{fg}$  is the gel-filler mass (g);  $W_t$  is the mass of the sample (g);  $m_f$  the

amount of charge on the compound (phr);  $m_r$  the amount of rubber in the compound (phr).

Elastomeric compounds characterization was carried out by rheometric properties obtained from a Tech Pro Rheotech OD+ (USA) oscillating disk rheometer, according to ASTM D5289-19a in an uncured sample of approximately 5 g, from the mixing of the roller mixer, at 160 °C, with an amplitude of 1° and a deformation frequency of 1.67 Hz for 30 minutes.

The cure rate index (CRI) was obtained from the rheometric curve data, according to Equation 2.

$$CRI = \frac{100}{t_{90} - t_{s1}} \quad (2)$$

Where CRI is the cure rate;  $t_{s1}$  the pre-vulcanization time (min) and  $t_{90}$  the optimal vulcanization time (min).

The rubbers taken from the two-roll mill were vulcanized by compression molding in a Shultz hydraulic press, model PHS 15 T (Brazil), at 160°C for a period corresponding to the optimum vulcanization time ( $t_{90}$ ) determined from the rheometric curve. Plates with dimensions 150 x 150 x 2 mm were prepared according to ASTM D3182-16. The samples were cut for the plates mechanical tests.

Tensile strength was evaluated according to ASTM D412-16 in an Emic universal testing machine, model DL-3000 (Brazil), with a force of 20 kN and a detachment speed of the claws of 50 mm.min<sup>-1</sup> on five samples. Tear strength was tested according to ASTM D624-00 in the same universal testing machine on five samples. Hardness testing (Shore A) was performed according to ASTM D2240-15 using a Teclock brand Shore A durometer, model GS709 (Japan), with 5 measurements of the property.

The one-way Analysis of Variance (ANOVA) method, with an alpha factor of 0.05 and a confidence level of 95%, was used to validate the significance of the hardness and tear strength results of the elastomeric compounds. For the variance calculation, a script was written in R language.

### 3. Results and Discussion

#### 3.1. Characterization of the biochar samples by instant analysis

Table 1 shows the results of the instant analysis of the biochar samples at pyrolysis temperatures of 400 °C (BIO400) and 900 °C (BIO900). In Table 1, it was found that the biochar produced at 900 °C presents lower volatile matter content and higher ash and solid carbon content than the biochar produced at 400 °C. The pyrolysis temperature has a significant effect on the physicochemical properties, as the volatile content decreases with the progression of thermal decomposition, and consequently increase the ash and

**Table 1.** Proximate analysis for biochars samples at temperatures of 400 and 900 °C of the pyrolysis process.

Sample	Moisture (wt%)	Volatile matter (wt%)	Ash (wt%)	Fixed carbon* (wt%)
BIO400	2.6	29.6	1.5	66.3
BIO900	2.9	3.3	2.7	91.1

\*Obtained by difference.

solid carbon content in the biochar<sup>19,20</sup>. These characteristics influence the reinforcement and affect the properties of the final compound, as the volatile content reflects the oxygen content and the polar component of the charge<sup>20,21</sup>.

### 3.2. Morphological characterization of biochar samples

Figure 2 shows SEM micrographs for samples of biochar produced at 400°C and 900°C.

It was possible to observe the development of pores and irregularities on the surface of the biochar by microscope analysis. The pyrolysis process naturally increases the porosity of the final product, and the temperature plays a significant effect on the porosity of the biochar, i.e., the increase in temperature leads to an increase in the porosity of the biochar, in addition to producing the irregularity of the surface of the biochar<sup>21,22</sup>. The irregularity of the surface of the filler is an important factor for reinforcement because it increases the reinforcing capacity of the material, regardless of the surface area, due to its direct influence on the surface free energy, increasing the filler-elastomer interaction<sup>23</sup>.

### 3.3. Surface area analysis by $N_2$ adsorption of biochar samples

The specific surface area ( $S_{\text{BET}}$ ), specific external surface area ( $S_{\text{EXT}}$ ), specific micropore area ( $S_{\text{MICRO}}$ ) and micropore volume ( $V_{\text{MICRO}}$ ) results for the biochars at the two temperatures of the pyrolysis process are presented in Table 2.

The surface analysis of the BIO400 and BIO900 biochars showed the small micropore area of the biochars after the ball milling process. Normally, the biochar produced at these temperatures (400 °C and 900 °C) presents a microporous area of about 20  $\text{m}^2 \cdot \text{g}^{-1}$  due to the correlation between the pyrolysis temperature and the surface area and microporosity due to the decomposition of lignocellulosic material, especially aromatic lignin, which eliminates volatile substances that block the pores<sup>24</sup>. At low temperatures ( $\leq 500^\circ\text{C}$ ), lignin is not converted into polycyclic aromatic hydrocarbons, making the biochar less hydrophobic<sup>25</sup>.

The increase in porosity makes the material ineffective for application as reinforcing filler in elastomeric compounds since the mechanical stability of the material is inverse to porosity<sup>26</sup>. According to Leblanc<sup>27</sup>, fillers with surface area smaller than 10  $\text{m}^2 \cdot \text{g}^{-1}$ , are considered inert fillers, as large areas compromise the mechanical properties of the compound.

### 3.4. Surface free energy analysis by the contact angle method of biochar samples

Table 3 presents the results for the contact angle ( $\theta$ ) for distilled water and toluene, the dispersive ( $\gamma_S^d$ ) and polar ( $\gamma_S^{SP}$ ) components and the surface free energy ( $\gamma_s$ ) for samples BIO400 and BIO900.

The filler surface free energy is an important parameter for a filler used to reinforce elastomers because it is related to the interaction between them and affects the properties of elastomeric compounds<sup>28</sup>. The particle size or the outer surface has an influence on the dispersive component of the free energy. The surface activity, i.e., the surface functional groups, mainly hydroxyl, affect the polar component<sup>29</sup>. The charge-charge interaction is related to the polar component; the higher the value of this property, the greater the charge-charge interaction<sup>30</sup>. Tensile strength has a positive dependence for the dispersive component and a negative dependence for the polar component<sup>31</sup>. The rebound decreases

**Table 2.** Textural properties of the biochars BIO400 e BIO900.

Samples	$S_{\text{EXT}}$ ( $\text{m}^2 \cdot \text{g}^{-1}$ )	$S_{\text{MICRO}}$ ( $\text{m}^2 \cdot \text{g}^{-1}$ )	$S_{\text{BET}}$ ( $\text{m}^2 \cdot \text{g}^{-1}$ )	$V_{\text{MICRO}}$ ( $\text{cm}^3 \cdot \text{g}^{-1}$ )
BIO400	2.01	0.86	2.87	0.007
BIO900	2.17	0.84	3.02	0.000

**Table 3.** Surface free energy and London dispersive component ( $\gamma_S^d$ ) and polar component ( $\gamma_S^{SP}$ ) of the biochars.

Samples	$\theta_{\text{water}}$ ( $^\circ$ )	$\theta_{\text{toluene}}$ ( $^\circ$ )	$\gamma_S^d$ ( $\text{mJ} \cdot \text{m}^{-2}$ )	$\gamma_S^{SP}$ ( $\text{mJ} \cdot \text{m}^{-2}$ )	$\gamma_s$ ( $\text{mJ} \cdot \text{m}^{-2}$ )
BIO400	120.4 $\pm$ 0.3	0.0	28.5	16.6	45.1
BIO900	128.6 $\pm$ 0.3	0.0	28.5	11.2	39.7

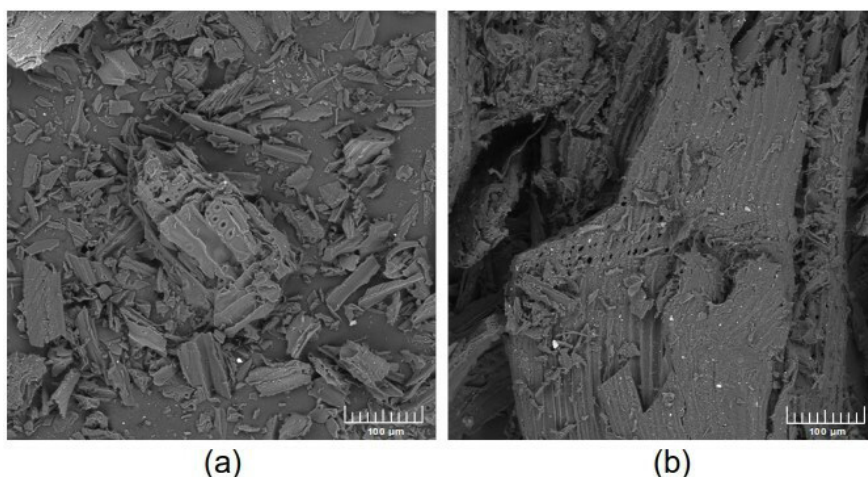


**Figure 2.** SEM micrograph of (a) biochar produced at 400 °C and (b) 900 °C with 500x magnitude.

with decreasing oxygen concentration at the surface of the charge because the C–C bond has a lower binding energy. The crosslink density and the modulus of elasticity are not affected by the oxygen concentration<sup>32</sup>.

The calculation of surface energy and its components for the biochar samples was performed based on the Fowkes method. The samples showed moderate values for the dispersive component, 28.5 mJ.m<sup>-2</sup> for the two biochars, and low values for the polar component, 16.6 mJ.m<sup>-2</sup> for BIO400 and 11.2 mJ.m<sup>-2</sup> for BIO900. Values above 40 mJ.m<sup>-2</sup> are considered high for both<sup>31</sup>. Comparing the results with other reinforcing fillers such as carbon black N550, the dispersive component is 45 mJ.m<sup>-2</sup> and 3 mJ.m<sup>-2</sup> for the polar component. The high dispersive component value leads to a large potential for material agglomeration, whose final structure is an agglomerate with an irregular shape, and since the interaction between the charges to form the structure results from weak forces, the structure breaks into a smaller structure called an aggregate due to shear during the production of the elastomeric compounds, the aggregate being the final form of the carbon black in the compounds<sup>28</sup>. Since the biochar samples did not show significant value in the polar and nonpolar components, the material showed low agglomeration potential, which consequently does not have a complex structure at any temperature, but a simple structure that does not provide reinforcement compatible with carbon black.

BIO900 sample showed greater hydrophobicity than BIO400, indicating a lesser interaction with polar compounds, observed by the higher contact angle shown in Figure 3. For toluene, a nonpolar liquid, the opposite occurred with the samples presenting an angle of 0°.

### 3.5. Characterization of mixtures and elastomeric compounds

#### 3.5.1. Bound rubber content

Table 4 presents data on the content of rubber bound to reinforcing filler for the elastomeric compounds of NR and NBR.

The data presented in Table 4 showed that biochar has a better interaction with polar elastomers than carbon black, with higher bound rubber content with NBR than with NR. Carbon black presents about 5% of its composition of oxygen groups, the remainder being carbon and hydrogen, showing better interaction with NR than the compounds with

biochar. The binding rubber content might increase by the interaction of the oxygenated groups on the charge surface (related to the volatile content) with the unsaturation of the polymer, normally at 100 °C<sup>33</sup>. In addition, the polarity of the charge and the elastomer also influences the content of bonded rubber<sup>34,35</sup>.

#### 3.6. Rheometric characterization of elastomeric compounds

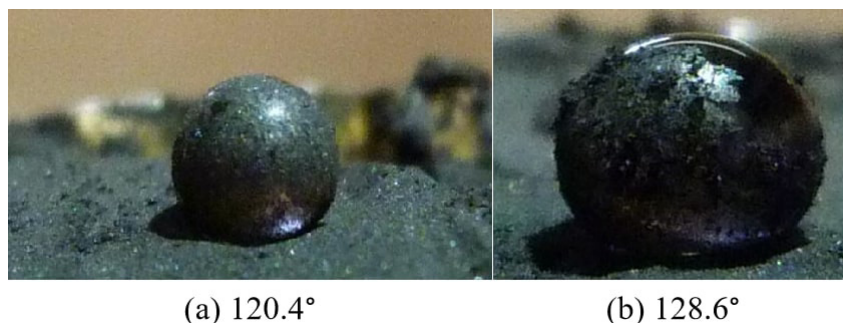
The rheometric characterization of the elastomeric compounds are presented in Table 5.

Table 5 shows the elastomeric compounds with biochar presented the lowest values of minimum torque ( $M_L$ ), evidencing a less irregular final structure of the filler concerning the compounds with carbon black, generating less occlusion of the rubber in the filler, indicated by the low viscosity<sup>36</sup>. The compounds with BIO400 showed a higher  $\Delta M$  than the BIO900 ones, regardless of the elastomer, indicative of the density of crosslinks.

NR/BIO900, NR/CB, NBR/BIO900, and NBR/CB compounds had lower values for optimum vulcanization time ( $t_{90}$ ) compared to the standard formulation, allowing the compounds to be produced in a shorter time, reducing energy and process costs, while NR/BIO400 and NBR/BIO400 had the longest vulcanization time compared to the standard formulation. This difference was attributed to the pH of the filler. Fillers with acidic pH prolong the vulcanization time due to adsorption of basic accelerators, and fillers with basic pH shorten the vulcanization time<sup>37</sup>. Pyrolysis temperature affects the pH of the biochar, the pH increases as the carbonization degree increases, temperatures above 400°C produce an alkaline pine biochar, and at temperatures below or equal to 400 °C, the pine biochar is

**Table 4.** Bound rubber content for NR and NBR based elastomeric compounds.

Compounds	Bound rubber (%)
NR/CB	17.8
NR/BIO400	11.6
NR/BIO900	6.7
NBR/CB	26.5
NBR/BIO400	81.2
NBR/BIO900	45.4



**Figure 3.** Contact angle with distilled water of samples of (a) BIO400 and (b) BIO900.

acidic, which confirms the vulcanization time data of the elastomeric compounds<sup>15,26</sup>.

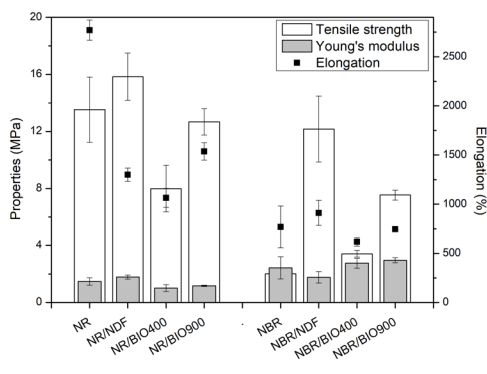
### 3.7. Mechanical characterization of elastomeric compounds

Table 6 presents the hardness results (Shore A) for the NR and NBR elastomeric compounds produced.

It was evidenced that all natural rubber formulations with the addition of biochar (NR/BIO400 and NR/BIO900) presented similar hardness to the formulation with carbon black (NR/CB). Although the values were close, the change in filler significantly affected the hardness results along the NR blends as can be evidenced by the ANOVA statistical analysis. The hardness of the compounds is determined by the interaction of the reinforcing filler with the elastomer, by the crosslink density and by the final structure formed by the reinforcing filler<sup>38</sup>. As for the elastomer compounds with NBR, similar to the NR compounds, the compounds with biochar showed better performance with a significant difference in the hardness results of the NBR compounds. This might be due to the better interaction of biochar with the elastomer, as biochar has a higher oxygen content (due to volatiles) and interacts better with polar elastomers. Although carbon black present lower interactions with the elastomer, the structural complexity formed along its aggregates works favourably, decreasing the polymer chains mobility and increasing the hardness of the compound<sup>35,36</sup>.

Figure 4 shows results of tensile strength, Young's modulus and elongation at break for NR and NBR elastomeric compounds.

Compared to the samples without reinforcing filler, the samples with biochar showed a reduction in tensile strength of about 69.2% for the blend NR/BIO400 and of about 6.8% for the blend NR/BIO900. When comparing the tensile strength with the blend with carbon black (NR/CB), the blend NR/BIO900 showed a similar value,  $12.7 \pm 0.9$  MPa,



**Figure 4.** Tensile strength, Young's modulus and elongation at break for NR and NBR compounds.

**Table 5.** Rheometric properties of NR and NBR elastomeric compounds.

Compounds	$M_L$ (dN.m)	$M_H$ (dN.m)	$\Delta M$ (dN.m)	$t_{S1}$ (min)	$t_{90}$ (min)	CRI ( $\text{min}^{-1}$ )
NR	2.8	15.5	12.7	3.4	8.2	20.8
NR/CB	7.4	30.5	23.1	1.4	6.5	19.4
NR/BIO400	1.1	20.2	19.1	3.8	10.1	15.9
NR/BIO900	2.2	16.6	14.3	2.8	5.4	38.9
NBR	2.6	15.0	13.1	4.4	9.2	20.9
NBR/CB	4.5	12.6	8.1	3.1	6.7	28.1
NBR/BIO400	3.8	14.8	11.1	4.4	11.9	13.5
NBR/BIO900	2.9	7.4	4.5	4.6	8.3	27.2

$M_L$  – minimum torque;  $M_H$  – maximum torque,  $\Delta M$  – cure rate index,  $t_{S1}$  – scorch time,  $t_{90}$  – optimum cure time.

**Table 6.** Hardness of NR and NBR elastomeric compounds developed and analysis of variance (ANOVA) for the filled compounds.

Compounds	Hardness (Shore A)			Compounds	Hardness (Shore A)		
NR	35 ± 1			NBR	49 ± 1		
NR/CB	52 ± 1			NBR/CB	67 ± 2		
NR/BIO400	50 ± 1			NBR/BIO400	65 ± 2		
NR/BIO900	47 ± 2			NBR/BIO900	68 ± 1		
ANOVA – Hardness NR							
Variation source	SQ	gl	MQ	F	P-value	F critical	Significance
Between groups	68.8	2	34.4	19.85	0.00016	3.885	yes
Within the groups	20.8	12	1.73				
Total	89.6	14					
ANOVA – Hardness NBR							
Variation source	SQ	gl	MQ	F	P-value	F critical	Significance
Between groups	18.53	2	9.27	4.41	0.037	3.89	yes
Within the groups	25.2	12	2.1				
Total	43.73	14					

SQ - sum of squares; gl - degrees of freedom; MQ - mean squares; F - F value of the F distribution.

**Table 7.** Tear resistance of NR and NBR elastomeric compounds and analysis of variance (ANOVA) for the filled compounds.

Compounds		Tear resistance (kN·m <sup>-1</sup> )					
NR		24.6 ± 2.6					
NR/CB		31.4 ± 3.8					
NR/BIO400		28.5 ± 3.8					
NR/BIO900		26.1 ± 2.8					
NBR		15.6 ± 2.6					
NBR/CB		59.7 ± 5.4					
NBR/BIO400		28.6 ± 2.3					
NBR/BIO900		38.0 ± 2.4					
ANOVA – Tear resistance NR							
Variation source	SQ	gl	MQ	F	P-value	F critical	Significance
Between groups	68.06	2	34.03	2.76	0.103	3.89	No
Within the groups	147.71	12	12.31				
Total	215.78	14					
ANOVA – Tear resistance NBR							
Variation source	SQ	gl	MQ	F	P-value	F critical	Significance
Between groups	2558.3	2	1279.16	95.57	9.19·10 <sup>-11</sup>	3.24	yes
Within the groups	160.6	12	13.38				
Total	2718.9	14					

compared to 15.8±1.7 MPa of the blend with carbon black. This result is due to the interaction between charge and elastomer, since the presence of oxygen along the charge increases the polar component, weakening the interaction with non-polar elastomers<sup>39-41</sup>.

The samples with biochar were shown to reinforce the NBR with an increase of 206.8% for the NBR/BIO400 blend and 275.2% for the NBR/BIO900 blend compared to the samples without reinforcement filler. In opposite to Leblanc<sup>27</sup>, according to which fillers with a specific surface area (BET) of less than 10 m<sup>2</sup>·g<sup>-1</sup> are considered inert fillers, the two types of biochar showed a reinforcing capacity, even for specific surface area of about 3 m<sup>2</sup>·g<sup>-1</sup>. This reinforcing capacity was attributed to the irregular surface of the biochar, as seen in the SEM microphotographs (Figure 1). After adsorption of the elastomer chains on the surface of the charge, the chains lose conformational entropy on an irregular surface, which is a smaller entropy loss than on a smooth surface because the chain can bypass the irregularity of the charge, providing to the compound greater reinforcement<sup>42-44</sup>. Compared to NBR/CB, the NBR/BIO900 and NBR/BIO400 compounds showed lower tensile strength, with a difference of 37.7% and 49.0%, respectively. Although the compounds have different chemical interactions and are much larger for the compounds with biochar, based on the results of the bonded rubber fraction, a high value for the dispersive component of the surface free energy is required for the charge-charge interaction to form a complex structure for the elastomer chains to adsorb in this structure, which is reflected in the increase in mechanical properties<sup>45,46</sup>.

The tear strength results for the NR elastomeric compounds are shown in Table 7.

Table 7 shows that the NR elastomeric compounds with biochar have higher values than the unfilled compound, about 6% and 16% higher for NR/BIO400 and NR/BIO900 compounds, respectively. When comparing NR/

CB, the tear strength results were alike, the change in filler did not affect the tear strength properties of the compounds from NR, presenting no statistical difference. Increasing the filler-elastomer interaction leads to an increase in the hardness of the compound and thus to a decrease in the tear strength<sup>47</sup>, which is controlled by the polarity of the filler and influenced by the surface<sup>48</sup>. For the NBR compounds, the ones with biochar had higher tear strength than the unfilled compound, showing that reinforcement occurs in the composite due to the filler-elastomer interaction. Compared with the NBR/CB compound, the compounds with biochar showed poorer results for this property. The dispersion of the reinforcing fillers in the polymer matrix and the amount of crosslinks formed during vulcanization are closely related to the increase in tear strength<sup>49</sup>. Therefore, the change in filler significantly affected the tear strength results in NBR compounds, as confirmed by ANOVA.

#### 4. Conclusion

The influence of temperature on the pyrolysis process of biomass shows that the higher temperature (900 °C) causes an increase in the concentration of fixed carbon and pH, and a decrease in the concentration of oxygen and polar component. At the lowest temperature (400 °C), the concentration of oxygen and polar component increases, while pH decreases. These parameters affect the rheometric properties, especially  $t_{90}$ , and the mechanical properties when it comes to rubber reinforcement. The temperature of 900 °C is the most promising for the production of biochar as a filler in elastomers.

#### 5. Acknowledgements

The authors would like to express their gratitude to CAPES-PROSUP and the support of the National Council

for Scientific and Technological Development (CNPQ) for the Productivity Research PQ2 scholarship.

## 6. References

- Habieb AB, Milani F, Milani G, Cerchiaro R. Rubber compounds made of reactivated EPDM for fiberreinforced elastomeric isolators: an experimental study. *Iran Polym J.* 2020;29(11):1031-43.
- Fan Y, Fowler GD, Zhao M. The past, present and future of carbon black as a rubber reinforcing filler - a review. *J Clean Prod.* 2020;247:119115.
- Zhang L, Zhang J, Liu H, Wu Q, Xiong H, Huang G, et al. Reinforcing self-healing and re-processable ionomers with carbon black: an investigation on the network structure and molecular mobility. *Compos Sci Technol.* 2021;216:109035.
- Hamm S, Hölscher K, Gruenberger TM, Moninot G, Örtel W, Petiniot N. Unsuitability of the zek/afps test method for the determination of polycyclic aromatic hydrocarbons in carbon black. *Rubber Chem Technol.* 2018;91(1):225-50.
- Okoye CO, Jones I, Zhu M, Zhang Z, Zhang D. Manufacturing of carbon black from spent tyre pyrolysis oil – a literature review. *J Clean Prod.* 2021;279:123336.
- Tunnicliffe LB. Fatigue crack growth behavior of carbon black– reinforced natural rubber. *Rubber Chem Technol.* 2021;94(3):494-514.
- Kopaczyk JM, Warguła J, Jelonek T. The variability of terpenes in conifers under developmental and environmental stimuli. *Environ Exp Bot.* 2020;180:104197.
- Jelonek Z, Drobniak A, Mastalerz M, Jelonek I. Emissions during grilling with wood pellets and chips. *Atmos Environ X.* 2021;12:100140.
- Amalina F, Razak ASA, Krishnan S, Zularisam AW, Nasrullah M. A comprehensive assessment of the method for producing biochar, its characterization, stability, and potential applications in regenerative economic sustainability – a review. *Clean Mat.* 2022;3:100045.
- Peterson SC. Copped biochars as partial replacement of carbon black filler in polybutadiene/natural rubber composites. *J Compos Sci.* 2020;4(4):147.
- El-Aziz MEA, Shafik ES, Tawfic ML, Morsi SMM. Biochar from waste agriculture as reinforcement filler for styrene/butadiene rubber. *Polym Compos.* 2022;43(3):1295-304.
- Peterson SC. Utilization of low-ash biochar to partially replace carbon black in styrene–butadiene rubber composites. *J Elastomers Plast.* 2013;45(5):487-97.
- Peterson SC, Chandrasekaran SR, Sharma BK. Birchwood biochar as partial carbon black replacement in styrene–butadiene rubber composites. *J Elastomers Plast.* 2016;48(4):305-16.
- Jiang C, Bo J, Xiao X, Zhang S, Wang Z, Yan G, et al. Converting waste lignin into nano-biochar as a renewable substitute of carbon black for reinforcing styrene-butadiene rubber. *Waste Manag.* 2020;102:732-42.
- Basu P. Biomass gasification and pyrolysis: practical design and theory. Amsterdam:Elsevier; 2010.
- Naghdi M, Taheran M, Brar SK, Rouissi T, Verma M, Surampalli RY, et al. A green method for production of nanobiochar by ball milling- optimization and characterization. *J Clean Prod.* 2017;164:1394-405.
- Park S, Kim J. Surface energy characterization of modified carbon blacks and its relationship to composites tearing properties. *J Adhes Sci Technol.* 2001;15(12):1443-52.
- Qian S, Huang J, Guo W, Wu C. Investigation of carbon black network in natural rubber with different bound rubber contents. *J Macromol Sci Part B Phys.* 2007;46(3):453-66.
- Štefanko AU, Leszczynska D. Impact of biomass source and pyrolysis parameters on physicochemical properties of biochar manufactured for innovative applications. *Front Energy Res.* 2020;8:138.
- Wu J, Wang L, Ma H, Zhou J. Investigation of element migration characteristics and product properties during biomass pyrolysis: a case study of pine cones rich in nitrogen. *RSC Adv.* 2021;11(55):34795-805.
- Zaitun Z, Halim A, Sadah Y, Cahyadi R. Surface morphology properties of biochar feedstock for soil amendment. *IOP Conf Ser Earth Environ Sci.* 2022;951(1):012034.
- Jiang Y, Wang X, Zhao Y, Zhang C, Jin Z, Shan S, et al. Effects of biochar application on enzyme activities in tea garden soil. *Front Bioeng Biotechnol.* 2021;9:728530.
- Tian C, Cui J, Ning N, Zhang L, Tian M. Quantitative characterization of interfacial properties of carbon black/elastomer nanocomposites and mechanism exploration on their interfacial interaction. *Compos Sci Technol.* 2022;222:109367.
- Tomczyk A, Sokółowska Z, Boguta P. Biochar physicochemical properties: pyrolysis temperature and feedstock kind effects. *Rev Environ Sci Biotechnol.* 2020;19(1):191-215.
- Chowdhury ZZ, Karim Z, Ashraf MA, Ashraf MA, Khalid K. Influence of carbonization temperature on physicochemical properties of biochar derived from slow pyrolysis of durian wood (*Durio zibethinus*) sawdust. *BioResources.* 2016;11(2):3356-72.
- Weber K, Quicker P. Properties of biochar. *Fuel.* 2018;217:240-61.
- Leblanc JL. Filled polymers: science and industrial applications. Boca Raton: CRC Press; 2010.
- Cha JH, Shin GJ, Kang MJ, Lee HI, Rhee KY, Park S-J. A study on the effect of electron acceptor-donor interactions on the mechanical and interfacial properties of carbon black/natural rubber composites. *Compos, Part B Eng.* 2018;136:143-8.
- Park SJ, Seo MK, Nah C. Influence of surface characteristics of carbon blacks on cure and mechanical behaviors of rubber matrix compoundings. *J Colloid Interface Sci.* 2005;291(1):229-35.
- Kohls DJ, Beaucage G. Rational design of reinforced rubber. *Curr Opin Solid State Mater Sci.* 2002;6(3):183-94.
- Kang MJ, Heo YJ, Jin FL, Park S-J. A review: role of interfacial adhesion between carbon blacks and elastomeric materials. *Carbon Lett.* 2016;18(0):1-10.
- Sweitzer CW, Burgess CW, Lyon F. The chemistry of carbon black in rubber reinforcement. *Rubber Chem Technol.* 1961;34(3):709-28.
- Dannenberg EM. The effects of surface chemical interactions on the properties of filler-reinforced rubbers. *Rubber Chem Technol.* 1975;48(3):410-44.
- Bandyopadhyay S, De PP, Tripathy DK, De SK. Influence of surface oxidation of carbon black on its interaction with nitrile rubbers. *Polymer.* 1996;37(2):353-7.
- Dannenberg EM. Bound rubber and carbon black reinforcement. *Rubber Chem Technol.* 1986;59(3):512-24.
- Hiranobe CT, Ribeiro GD, Torres GB, Reis EAP, Cabrera FC, Job AE, et al. Cross-linked density determination of natural rubber compounds by different analytical techniques. *Mater Res.* 2021;24(Suppl. 1):e20210041.
- Blokh GA, Melamed CL. The interaction of carbon black with sulfur, MBT and TMTD in vulcanization. *Rubber Chem Technol.* 1961;34(2):588-99.
- Roberts AD. Rubber surface oxidation effect on wet friction. *Rubber Chem Technol.* 2020;93(1):63-78.
- Sadeghi M, Malekzadeh M, Taghvaei-Ganjali S, Motiee F. Correlations between natural rubber protein content and rapid predictions of rheological properties, compression set and hardness of rubber compound. *J Indian Chem Soc.* 2021;98(11):100162.
- Mostafa A, Abouel-Kasem A, Bayoumi MR, El-Sebaie MG. Rubber-filler interactions and its effect in rheological and mechanical properties of filled compounds. *J Test Eval.* 2010;38(3):347-59.
- Robertson CG, Hardman NJ. Nature of carbon black reinforcement of rubber: perspective on the original polymer nanocomposite. *Polymers.* 2021;13(4):538.

42. Schröder A, Klüppel M, Schuster RH. Characterization of surface activity of carbon black and its relation to polymer-filler interaction. *Macromol Mater Eng.* 2007;292(8):885-916.
43. Zedler L, Colom X, Cañavate J, Saeb MR, Haponiuk JT, Formela K. Investigating the impact of curing system on structure-property relationship of natural rubber modified with brewery by-product and ground tire rubber. *Polymers.* 2020;12(3):545.
44. Pazur RJ, Mengistu T. Activation energies of thermo-oxidized nitrile rubber compounds of varying acrylonitrile content. *Rubber Chem Technol.* 2019;92(1):129-51.
45. Gholami F, Tomas M, Gholami Z, Mirzaei S, Vakili M. Surface characterization of carbonaceous materials using inverse gas chromatography: a review. *Electrochem.* 2020;1(4):367-87.
46. Zhang Y, Park SJ. Effect of mercapto-terminated silane treatment on rheological and mechanical properties of rice bran carbon-reinforced nitrile butadiene rubber composites. *Macromol Res.* 2018;26(5):446-53.
47. Xie T, Wang F, Xie C, Lei S, Yu S, Liu J, et al. Mechanical properties of natural rubber filled with foundry waste derived fillers. *Materials.* 2019;12(11):1863.
48. Costa HM, Visconte LLY, Nunes RCR, Furtado CRG. Rice husk ash filled natural rubber compounds – the use of rheometric data to qualitatively estimate optimum filler loading. *Int J Polym Mater.* 2004;53(6):475-97.
49. Fu W, Wang L, Huang J, Liu C, Peng W, Xiao H, et al. Mechanical properties and mullins effect in natural rubber reinforced by grafted carbon black. *Adv Polym Technol.* 2019;2019:1-11.